Colloid Polym Sci 274:705–716 (1996)

ORIGINAL CONTRIBUTION

A. Ziabicki

Crystallization of polymers in variable external conditions.

II. Effects of cooling in the absence of stress and orientation

Received: 31 May 1996
Accepted: 10 January 1996

Dr. A. Ziabicki (✉)
Polish Academy of Sciences
Institute of Fundamental Technological Research
21 Swietokrzyska St.
00-049 Warszawa, Poland

Abstract General equations of crystallization in variable conditions derived in the former paper [1] have been applied to non-isothermal crystallization of unstressed and unoriented polymers. Crystallization rate involving transient and athermal effects is controlled by temperature, T, and cooling rate, $\dot{T}$. Experimental procedures leading to determination of three temperature-dependent material functions: steady-state crystallization rate, $\mathscr{K}_{st}(T)$, relaxation time, $\tau(T)$, and athermal nucleation function, $Z(T)$, are outlined.

Key words Nucleation theory – non-isothermal crystallization – thermal nucleation – athermal nucleation – relaxation time

General equations of non-isothermal crystallization

In ref. [1] a new model of crystallization kinetics in variable external conditions has been developed. The model takes into account transient and athermal effects, and a variety of time-dependent external conditions. Variable temperature, T, pressure, p, stress, σ, and other conditions form time-dependent vector of external conditions

$$\Psi(t) = \{T(t), p(t), \sigma(t), \dots\} . \tag{1}$$

The terms "isothermal" and "non-isothermal" are used in a general sense, and concern variations of all conditions characterized by the vector $\Psi(t)$.

The model is based on the modified Kolmogoroff–Avrami–Evans treatment of phase transitions [2–5]. Along with the linear measure of the degree of transformation, i.e., volume fraction of the crystallized material

$$x(t) = v_{cr}/v_{tot} \in (0, 1) \tag{2}$$

a non-linear measure is used

$$P(t) = [-\ln(1 - x(t))]^{1/m} \in (0, \infty) \tag{3}$$

m is a model constant, which in isothermal conditions reduces to the Avrami exponent. The non-linear transformation (crystallization) rate,

$$\mathscr{K}(t) = dP/dt \propto t_{\frac{1}{2}}^{-1} \tag{4}$$

a function of time and time-dependent conditions $\Psi(t)$, in the isokinetic approximation reduces to crystallization half-period, $t_{\frac{1}{2}}$.

In variable external conditions, $\mathscr{K}(t)$ is a sum of thermal and athermal contributions, and can be presented in the form [1]

$$\mathscr{K}(t, \Psi(t)) = \mathscr{K}_{th}(t, \Psi) + \mathscr{K}_{ath}(t, \Psi, \dot{\Psi}) = \mathscr{K}_{th}[1 + \dot{\Psi} \cdot Z(t, \Psi(t))]^{\mu} \tag{5}$$

Z, a vector in the space of conditions Ψ, characterizes athermal nucleation. The exponent μ depends on whether athermal mechanism affects nucleation and growth, or only one of these processes.

Thermal contribution to crystallization rate results as an integral

$$\mathscr{K}_{th}(t, \Psi) = e^{-\xi}\left[\mathscr{K}_0 + \int_0^{\xi} e^{\xi'} \mathscr{K}_{st}[\Psi(\xi')]\, d\xi'\right], \tag{6}$$

Colloid & Polymer Science, Vol. 274, No. 8 (1996)

where

$$\xi(t) = \int_0^t \frac{dt'}{\tau[\Psi(t')]} \tag{7}$$

$\tau(\Psi)$ is relaxation time, and $\mathscr{K}_{st}(\Psi)$ – steady-state crystallization rate, both functions of external conditions. Equations (5)–(7) provide a basis for the general model of non-isothermal crystallization.

Non-isothermal crystallization controlled by temperature

In this paper we consider a simple case of non-isothermal crystallization in which the vector of external conditions, Ψ, has only one component – temperature, T

$$\Psi(t) \to T(t) . \tag{8}$$

Temperature distribution is assumed uniform

$$\nabla T = 0 . \tag{9}$$

All vector and tensor characteristics appearing in the general model reduce to scalar functions of temperature, T. This yields crystallization rate controlled by thermal nucleation in the form

$$\mathscr{K}_{th}(t, T(t)) = e^{-\xi}\left[\mathscr{K}_0 + \int_{T(0)}^{T(t)} \frac{e^{\xi}\mathscr{K}_{st}(T')\,dT'}{\tau(T')\dot{T}}\right] . \tag{10}$$

We assume that athermal effects are present only in primary nucleation, while growth is controlled by a pure thermal mechanism. This leads to $\mu = 1/(n+1)$, where n denotes dimensionality of growth, and athermal function, $Z(T)$ is a characteristic of three-dimensional primary nucleation ($Z = Z_3$). The total crystallization rate from Eq. (4) reduces to

$$\mathscr{K}(t, T(t), \dot{T}(t)) = \mathscr{K}_{th}(t, T(t))\,[1 + \dot{T}\cdot Z_3]^{1/(n+1)}$$

$$= e^{-\xi}\left[\mathscr{K}_0 + \int_{T(0)}^{T(t)} \frac{e^{\xi}\mathscr{K}_{st}(T')\,dT'}{\tau(T')\dot{T}}\right][1 + \dot{T}\cdot Z_3]^{1/(n+1)} . \tag{11}$$

In Eqs. (10) and (11) unique relation between time and temperature has been assumed, and T is taken as the integration variable. The variable ξ, expressed as an integral over temperature, reads

$$\xi(t) = \int_0^t \frac{dt'}{\tau[T(t')]} \to \xi(T) = \int_{T(0)}^{T(t)} \frac{dT'}{\tau(T')\dot{T}} . \tag{12}$$

The integral in Eq. (10) representing thermal crystallization rate can be expanded in a series of cooling rates. We introduce a dimensionless cooling rate variable

$$u \equiv \tau\dot{T}/T = \tau\cdot(d\ln T/dt) = d\ln T/d\xi \tag{13}$$

which yields

$$e^{-\xi}\int \frac{e^{\xi}\mathscr{K}_{st}(T')\,dT'}{\tau(T')\dot{T}} = \mathscr{K}_{st}(T) - u\,[d\mathscr{K}_{st}/d\ln T]$$

$$+ u^2[d^2\mathscr{K}_{st}/d\ln T^2 + (d\mathscr{K}_{st}/d\ln T)\,(d\ln u/d\ln T)]$$

$$- u^3[d^3\mathscr{K}_{st}/d\ln T^3 + 3(d^2\mathscr{K}_{st}/d\ln T^2)\,(d\ln u/d\ln T)$$

$$+ (d\mathscr{K}_{st}/d\ln T)\,(d^2\ln\dot{T}/d\ln T^2 + d^2\ln\tau/d\ln T^2$$

$$+ 2(d\ln u/d\ln T)^2)] + u^4[\cdots] + \cdots \tag{14}$$

where

$$d\ln u/d\ln T = d\ln\dot{T}/d\ln T + d\ln\tau/d\ln T - 1 . \tag{14a}$$

When crystallization follows prolonged heating, the integration constant

$$C = \mathscr{K}_0 - [\mathscr{K}_{st} - u(d\mathscr{K}_{st}/d\ln T) + \cdots]_{T=T_0} \tag{15}$$

is small and can be neglected.

The ratio of athermal to thermal nucleation is proportional to cooling rate and relaxation time (cf. Appendix). For three-dimensional primary nucleation

$$(\dot{N}_{ath}/\dot{N}_{th})_3 = \dot{T}\cdot Z_3 = u\cdot A_3(T) \tag{16}$$

and A_3 is a material characteristic.

The total crystallization rate can be expanded in a series of the dimensionless cooling rate variable u, and presented in the form

$$\mathscr{K}(t) - Ce^{-\xi}[1 + uA_3(T)]^{1/(n+1)}$$

$$= \mathscr{K}_{st}(T)\,[1 + F_1u + F_2u^2 + F_3u^3 + \cdots] . \tag{17}$$

The coefficients F_i are functions of temperature

$$F_1(T) = -\frac{\partial\ln\mathscr{K}_{st}}{\partial\ln T} + \frac{1}{n+1}A_3(T) \tag{18}$$

$$F_2(T) = \frac{\partial^2\ln\mathscr{K}_{st}}{\partial\ln T^2} + \frac{\partial\ln\mathscr{K}_{st}}{\partial\ln T}(d\ln u/d\ln T)$$

$$+ \left(\frac{\partial\ln\mathscr{K}_{st}}{\partial\ln T}\right)^2 + \frac{1}{n+1}A_3\left(\frac{\partial\ln\mathscr{K}_{st}}{\partial\ln T} + \frac{1}{2}\frac{n}{n+1}A_3\right) . \tag{19}$$

The expansion (17) provides a convenient form of describing crystallization rate at slow cooling. At $u \to 0$, Eq. (17) yields quasi-static model of non-isothermal crystallization [6]

$$\mathscr{K}(t) \to \mathscr{K}_{th}(t) \to \mathscr{K}_{st}[T(t)] \tag{20}$$

and in steady-state isothermal conditions, reduces to the Avrami constant, K_m

$$\mathscr{K}(t) \to \mathscr{K}_{st}(T) = K_m^{1/m} = \text{const.} \tag{21}$$

Temperature-dependent crystallization rate characteristics

In principle, kinetic characteristics of crystallization can be derived from the theory of nucleation. Both, primary nucleation and nucleation-controlled growth can be described by physical equations [7, 8]. In the Appendix we show basic equations of the nucleation theory, used for derivation of the steady-state crystallization rate, and the athermal nucleation function.

Steady-state, isothermal crystallization rate, as defined in Eq. (4) is composed of nucleation, and growth characteristics. For n-dimensional growth (with linear growth rate $\dot{R}$) of N_0 pre-determined nuclei

$$\mathscr{K}_{st}(T) = [N_0(\dot{R}(T))^n]^{1/n} = N_0^{1/n}\,\dot{R}(T) \tag{22}$$

and for sporadic nucleation rate $\dot{N}_{th}$ followed by n-dimensional growth

$$\begin{aligned}\mathscr{K}_{st}(T) &= [\dot{N}_{th}(T)(\dot{R}(T))^n]^{1/(n+1)} \\ &= \dot{N}_{th}(T)^{1/(n+1)}(\dot{R}(T))^{n/(n+1)}\,.\end{aligned} \tag{23}$$

Identifying $\dot{N}_{th}$ in Eq. (23) with $\dot{N}_{th,st,3}$ derived in the Appendix, assuming linear growth rate proportional to the two-dimensional nucleation rate

$$\dot{R}(T) = R_0\,\dot{N}_{th,st,2}(T) \tag{24}$$

and assuming the same relaxation time for primary nucleation and growth, we obtain the following expressions for isothermal, steady-state crystallization rate

$$\mathscr{K}_{st}(T) = N_0^{1/n} R_0 K_2 (T\Delta T/T_m^2)\exp[-E_a/kT] \times \exp\left[\frac{-C_2 T_m^2}{T\Delta T}\right] \tag{25}$$

for growth of predetermined nuclei, and

$$\mathscr{K}_{st}(T) = (R_0 K_2)^{n/(n+1)} K_3^{1/(n+1)} (T\Delta T/T_m^2)\exp[-E_a/kT] \times \exp\left[\frac{-nC_2 T_m^2}{(n+1)T\Delta T}\right]\exp\left[\frac{-C_3 T_m^3}{(n+1)T\Delta T^2}\right] \tag{26}$$

for sporadic nucleation and growth. The appropriate constants are given in the Appendix (Table A1).

Temperature dependence of relaxation times is often presented in the Arrhenius form

$$\tau = \tau_0 \exp[E_a/kT] \tag{27}$$

with constant activation energy, E_a, or as a semi-empirical Williams–Landel–Ferry (WLF) equation [11]

$$\tau = \tau(T_g)\exp\left[\frac{-17.44(T - T_g)}{T - T_g + 51.6}\right] \tag{28}$$

T_g denotes glass transition temperature.

Assuming that athermal effects appear only in the primary nucleation, we will use athermal correction for three-dimensional nucleation (cf. Appendix, Eq. A25).

$$(\dot{N}_{ath,st}/\dot{N}_{th,st})_3 \equiv \dot{T}\cdot Z_3 \equiv u\cdot A_3\,. \tag{29}$$

The material function $A_3(T)$ results in the form

$$\begin{aligned}A_3(T) &\simeq -\frac{8(c_3\sigma_3 T_m)^4}{9(D_{0.3}/T)\Delta h^4(\Delta T)^5 v_0^{4/3}} \\ &\simeq -\frac{8hc_3^3(\sigma_3 T_m)^4}{9k\tau_0\Delta h^4(\Delta T)^5 v_0^{4/3}}\,.\end{aligned} \tag{30}$$

The ratio $(D_{0.3}/T)$ is independent of temperature, if absolute reaction rate theory (Eq. A8) is applied. Below the melting temperature, T_m, A_3 is negative, and the athermal correction $(u\cdot A_3)$ is positive whenever cooling is applied $(\dot{T} < 0)$.

Quantitative evaluation of Eqs. (22)–(30) requires the knowledge of many parameters, such as melting temperature, glass transition temperature, heat of fusion, interface tensions, molecular volume of the kinetic element, transport activation energy, relaxation time(s), variables describing geometry of clusters (c_2, c_3, R_0), growth diffusion coefficients, concentration of predetermined nuclei, dimensionality of crystal growth, etc. Not all of these parameters are known, and values of those characteristics which have been measured (Δh, σ_g, σ_e, T_m), scatter in a wide range, dependently on the sample and measuring technique. Geometrical parameters are usually subject to assumption, and so are diffusion coefficients $D_{0.2}$, $D_{0.3}$.

Nucleation theory itself involves many simplifications which limit its applicability to a narrow range of conditions. Linear dependence of the free energy of aggregation on temperature (Eq. A1) is justified only in the vicinity of thermodynamic equilibrium, i.e., for small undercooling. Applicability of the theory of chemical reactions to the "growth diffusion" coefficient $\mathscr{D}_{gr}(T)$ can be questioned. All this makes application of the nucleation theory with *a priori* determined material parameters, impractical, if quantitative description of crystallization is sought.

Colloid & Polymer Science, Vol. 274, No. 8 (1996)

Crystallization rate characteristics derived from the nucleation theory can provide a basis for qualitative discussion. We will present such an analysis in one of the following sections. For quantitative description of technological processes where external conditions change in a wide range, another approach must be used. Basic kinetic characteristics $\mathscr{K}_{st}(T)$, $\tau(T)$, $A_3(T)$, will be postulated as empirical functions with a small number of parameters, and the latter will be determined for each material by direct experiments. The form of empirical functions should be consistent with theoretical (physical) predictions and should describe the correct asymptotic behaviour.

The equation for temperature-dependent crystallization rate, may be postulated in the form, derived from the nucleation theory (cf. Appendix)

$$\mathscr{K}_{st}(T) = \text{const}_1 \cdot (T\Delta T/T_m^2)\exp[-E_a/kT] \times \exp\left[\frac{-\text{const}_2 \cdot T_m^2}{T\Delta T}\right]\exp\left[\frac{-\text{const}_3 \cdot T_m^3}{T(\Delta T)^2}\right]. \quad (31)$$

Quantitative evaluation of Eq. (31) requires the knowledge of const_1, const_2, const_3, melting temperature, T_m, (appearing in the undercooling), and activation energy, E_a.

For qualitative theoretical analysis, the constants in Eq. (31) can be related to physical parameters of the nucleation theory (see Table A1 in the Appendix). Assuming that crystallization involves n-dimensional growth of N_0 pre-determined nuclei, we obtain

$$\begin{aligned}\text{const}_1 &= N_0^{1/n} R_0 K_2 \\ \text{const}_2 &= C_2 \\ \text{const}_3 &= 0\,.\end{aligned} \quad (32)$$

In the case of sporadic nucleation followed by n-dimensional growth, we have

$$\begin{aligned}\text{const}_1 &= (R_0 K_2)^{n/(n+1)} K_3^{1/(n+1)} \\ \text{const}_2 &= nC_2/(n+1) \\ \text{const}_3 &= C_3/(n+1)\,.\end{aligned} \quad (33)$$

Some parameters: R_0, $C_{0,2}$, $C_{0,3}$ (included in K_2 and K_3), are not defined by known physical parameters.

An approach alternative to Eq. (31), consists in fitting experimental data with purely empirical equations. The present author [6] postulated for this purpose a Gaussian function. The function should be truncated in the range where crystallization is excluded for thermodynamic ($T > T_m$), or kinetic reasons ($T < T_g$)

$$\mathscr{K}_{st}(T) = \begin{cases}\mathscr{K}_{max}\exp[-4\ln 2(T - T_{max})^2/D_{\frac{1}{2}}^2] & \text{for } T_m < T < T_g \\ 0 \quad \text{for } T > T_m, \text{ or } T < T_g\end{cases} \quad (34)$$

The material constants appearing in Eq. (34) have been compiled for several polymers in ref. [12]. Two examples are shown in Table 1 below.

Relaxation time, $\tau(T)$ will be postulated in the Arrhenius form, Eq. (27), with two adjustable constants, τ_0, and E_a. Constant, but adjustable activation energy seems to offer more flexibility for fitting experimental data than the WLF formula (Eq. 28), where activation energy is uniquely determined by glass transition temperature, T_g.

The fact that maximum crystallization rate temperature, T_{max}, and maximum crystallization rate, $\mathscr{K}_{max}$ are known for many polymers, makes possible refinement of the ill-defined parameter const_1 in Eq. (31). Substitution of experimentally determined coordinates of the maximum crystallization rate, $(\mathscr{K}_{max}, T_{max})$, eliminates four parameters: $C_{0,2}$, $C_{0,3}$, R_0, and τ_0.

The athermal nucleation correction is postulated in the form derived from the nucleation theory (Eq. 30) with an adjustable material constant const_4

$$A_3(T) = -\text{const}_4 \cdot (T_m/\Delta T)^5\,. \quad (35)$$

Experimental determination of the kinetic characteristics

Steady-state crystallization rate and relaxation times can be obtained in a series of standard, isothermal crystallization runs performed at different (constant) temperatures. Crystallization experiments should follow prolonged heating above T_m. Such a treatment, simulating conditions occurring in technological processes, is intended to destroy ordered structures possibly existing in the polymer prior to crystallization and to reduce the constant C in Eq. (15). In isothermal conditions athermal effects disappear, and time effects are confined to relaxation

$$\mathscr{K}(t; T) = (\mathscr{K}_0 - \mathscr{K}_{st}(T))e^{-t/\tau} + \mathscr{K}_{st}(T)\,. \quad (36)$$

Steady state crystallization rate at each temperature, may be obtained from the asymptotic behaviour at $t \to \infty$

$$\mathscr{K}_{st}(T) = \lim_{t\to\infty} \mathscr{K}(t; T) \quad (37)$$

and relaxation time, τ, from the slope

$$[\tau(T)]^{-1} = d\ln[\mathscr{K}_{st}(T) - \mathscr{K}(t; T)]/dt\,. \quad (38)$$

Determination of the athermal function $A_3(T)$, requires nonisothermal experiments performed at constant cooling rate.

Consider a series of crystallization runs covering the entire range of crystallization temperatures, i.e. starting at (or above) the melting temperature, T_m, and ending at (or

below), glass transition temperature, T_g. Crystallization experiments should be performed at different, but constant cooling rates. For each run, end value of crystallinity, P_∞, is determined, and entire set of data forms a function, $P_\infty(\dot{T})$.

In the discussed model, P_∞ is determined by the integral

$$P_\infty(\dot{T}) = [-\ln(1-x_\infty)]^{1/m} = \int_{t(T_m)}^{t(T_g)} \mathscr{K}(t;\dot{T})\,dt = -\frac{1}{\dot{T}}\int_{T_g}^{T_m} \mathscr{K}(T;\dot{T})\,dT\,. \tag{39}$$

Using the expansion (17), we obtain

$$-\dot{T}\cdot P_\infty(\dot{T}) = \int_{T_g}^{T_m} \mathscr{K}_{st}(T)\,dT + \dot{T}\int_{T_g}^{T_m} \mathscr{K}_{st}(F_1\tau/T)\,dT + \dot{T}^2\int_{T_g}^{T_m} \mathscr{K}_{st}(F_2\tau^2/T^2)\,dT + \cdots\,. \tag{40}$$

When the process is quasi-static, the product $(\dot{T}\cdot P_\infty)$ reduces to a material constant

$$\lim_{\dot{T}\to 0}(\dot{T}\cdot P_\infty) = -\int_{T_g}^{T_m} \mathscr{K}_{st}(T)\,dT = \text{const.} \tag{41}$$

First derivative with respect to $\dot{T}$

$$-d(\dot{T}\cdot P_\infty)/d\dot{T} = \int_{T_g}^{T_m} \mathscr{K}_{st}(F_1\tau/T)\,dT + 2\dot{T}\int_{T_g}^{T_m} \mathscr{K}_{st}(F_2\tau^2/T^2)\,dT + \cdots \tag{42}$$

taken in the limit $\dot{T}=0$, with F_1 from Eq. (18) and athermal function, $A_3(T)$ from Eq. (35) yields

$$\text{const}_4 = (n+1)\,T_m^{-5}\left[\lim_{\dot{T}\to 0}\frac{d(\dot{T}\cdot P_\infty)}{d\dot{T}} - \int_{T_g}^{T_m}(\partial\mathscr{K}_{st}/\partial T)\,\tau\,dT\right] \Big/ \int_{T_g}^{T_m}\frac{\mathscr{K}_{st}}{T\,\Delta T^5}\,\tau\,dT\,. \tag{43}$$

In the last integral in Eq. (43) there appears a weak singularity, when T approaches T_m: both, $\mathscr{K}_{st}$ in the numerator (exponentially) and ΔT in the denominator (linearily) approach zero. The singularity can be removed by integrating in the limits $(T_g, T_m-\varepsilon)$.

Using Eqs. (37), (38) and (43), all three material functions, $\mathscr{K}_{st}(T)$, $\tau(T)$, $A_3(T)$ can be obtained from direct experiments. The dimensionality exponent, n, must be assumed, or treated as an adjustable constant.

Numerical testing

Input data

We will test non-isothermal crystallization effects for *isotactic polypropylene* (i-PP) and *polyethylene terephthalate* (PET). Isothermal crystallization rate will be approximated with the truncated Gaussian function (Eq. (34)), and relaxation time with the Arrhenius equation (Eq. (27)). The material data used for testing are listed in Table 1.

Molecular parameters of the nucleation theory (Δh, σ_s, σ_e, T_m, etc.) are derived from isothermal crystallization [13, 14]. Parameters of the empirical crystallization rate function (Eq. 34), have been collected in ref. [12] from

Table 1 Nucleation and crystallization characteristics for isotactic polypropylene and polyethylene terephthalate

Data	i-PP	ref.	PET	ref.
heat of fusion, $\Delta h\times 10^{-9}$ erg/cm^3	1.4	[13]	1.8	[14]
interface tension, (side) σ_s, erg/cm^2	10	[13]	10.2	[14]
interface tension, (end) σ_e, erg/cm^2	122	[13]	190	[14]
$\sigma_3=(\sigma_s^2\sigma_e)^{1/3}$, erg/cm^2	23	[13]	27	[14]
molecular volume of a single kinetic element, $v_0\times 10^{22}$ cm^3	1.5		5.86	
melting temperature, T_m, K	481.2	[13]	553	[15]
glass transition temp., T_g, K	253	[16]	343	[15]
max. cryst. rate, K_{max}, s^{-1}	0.55	[12, 16]	0.016	[12, 15]
max. cryst. temperature, T_{max}, K	338.2	[12, 16]	463.2	[12, 15]
half-width of the cryst. rate-temperature curve, $D_{\frac{1}{2}}$, deg	30	[12, 16]	32	[12, 15]
relaxation time $\tau_0\times 10^6$, s	1.72	[17]	333	
activation energy, kJ/mole	76.8	[17]	54.8	[19]
athermal constant, $A_3\times 10^{11}$ (calculated from Eq. 28)	10178		5.166	

Colloid & Polymer Science, Vol. 274, No. 8 (1996)

experimental data [15, 16]. Relaxation time for polypropylene has been based on our recent study of memory effects in isothermal crystallization [17]. It is not certain that so calculated (rather long) relaxation times are relevant for crystallization kinetics. At the present moment we do not see any better source of the $\tau(T)$ function, though. Activation energy for polypropylene (from crystallization memory) was reasonably consistent with that from diffusion in the melt [18], or melt viscosity. For PET, activation energy has been taken from viscosity data [19], and the pre-exponential factor τ_0, arbitrarily adjusted so, that relaxation time in the temperature of melting is 50 s.

Figure 1 presents steady-state crystallization rate, $\mathscr{K}_{st}(T)$ from Eq. (34) and relaxation time, $\tau(T)$ for both polymers.

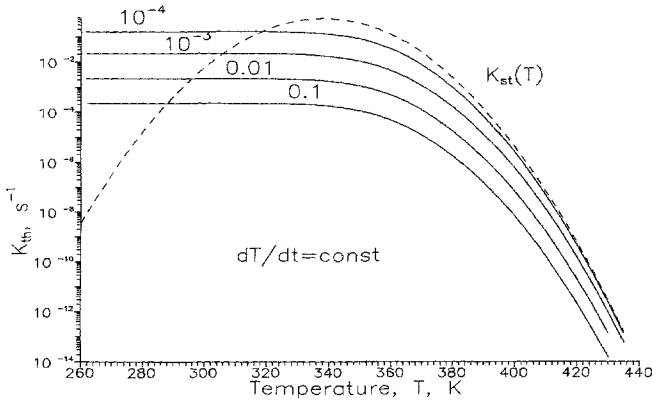

Fig. 2 Thermal crystallization rate, $\mathscr{K}_{th}(T, \dot{T})$ for polypropylene, vs. temperature. Constant cooling rates, $|\dot{T}|$, (deg/s) indicated

Relaxation effects in thermal crystallization

Figures 2 and 3 present thermal crystallization rate, calculated from Eq. (10) for polypropylene and PET. The process is assumed to start at T_m, and the integration constant, K_0 in Eq. (10) is assumed to be zero.

Solid lines in Figs. 2 and 3 describe thermal crystallization rates, $\mathscr{K}_{th}(T, \dot{T})$, dependent on temperature and cooling rate. Dashed lines represent steady-state values, $\mathscr{K}_{st}(T)$. The same data, reduced by $\mathscr{K}_{st}$ are shown in Figs. 4 and 5. It is evident that, with increasing cooling rate, actual crystallization rates deviate from steady-state values, and the more so, the higher is $|\dot{T}|$. In the range of high crystallization temperatures ($T > T_{max}$) steady-state crystallization rate increases as the polymer is cooled down. The increase of actual crystallization rate, however, lags behind that of $\mathscr{K}_{st}$. Below T_{max}, steady-state crystallization rate decreases, but the reduction is slower.

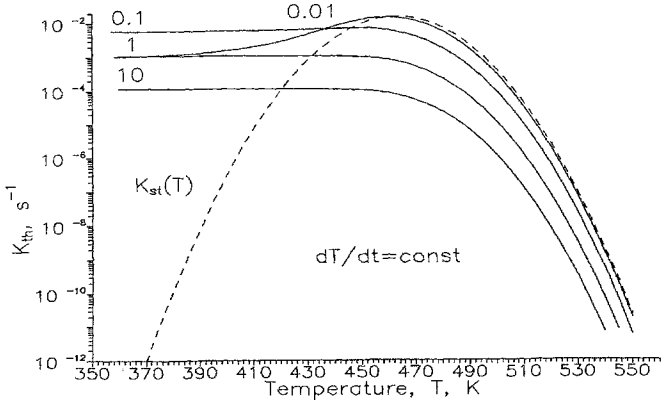

Fig. 3 Thermal crystallization rate, $\mathscr{K}_{th}(T, \dot{T})$ for polyethylene, terephthalate, vs. temperature. Constant cooling rates, $|\dot{T}|$, (deg/s) indicated

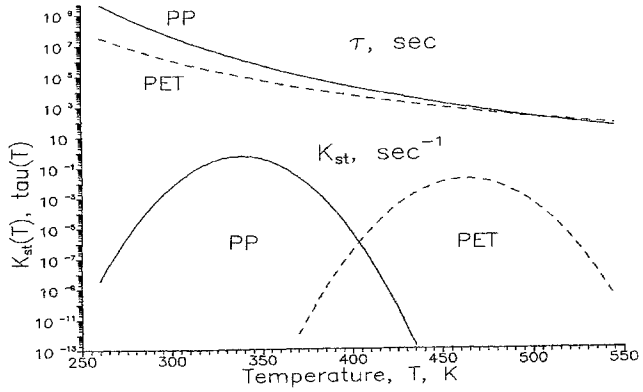

Fig. 1 Steady-state crystallization rate, $\mathscr{K}_{st}$, and relaxation time, τ, for isotactic polypropylene and polyethylene terephthalate, vs, temperature, T

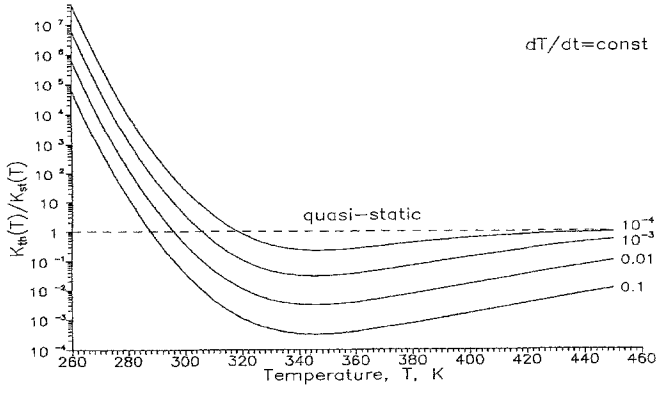

Fig. 4 The ratio of thermal crystallization rate to steady-state crystallization rate, $\mathscr{K}_{th}(T, \dot{T})/\mathscr{K}_{st}(T)$ for polypropylene, vs. temperature. Constant cooling rates, $|\dot{T}|$, (deg/s) indicated

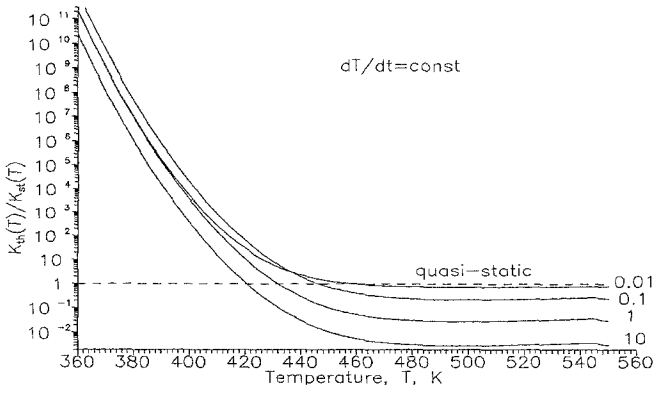

Fig. 5 The ratio of thermal crystallization rate to steady-state crystallization rate, $\mathscr{K}_{th}(T, \dot{T})/\mathscr{K}_{st}(T)$ for polyethylene terephthalate, vs. temperature. Constant cooling rates, $|\dot{T}|$, (deg/s) indicated

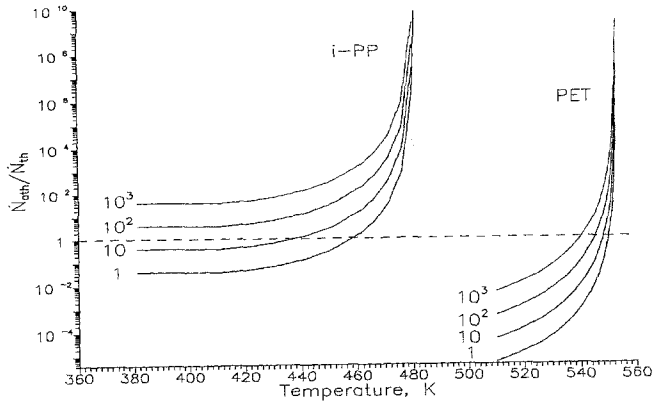

Fig. 6 The ratio of athermal to thermal nucleation rate, $\dot{N}_{ath}/\dot{N}_{th}$ for polypropylene and polyethylene terephthalate, vs. temperature. Constant cooling rates, $|\dot{T}|$, (deg/s) indicated

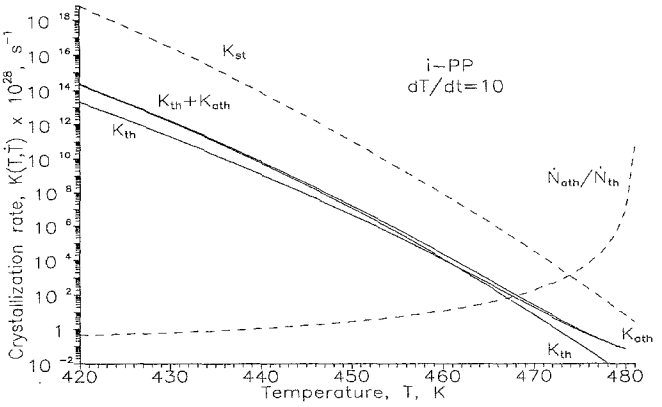

Fig. 7 Steady-state, thermal, athermal, and total crystallization rate components for polypropylene, in the vicinity of melting temperature. Cooling rate, $|\dot{T}| = 10$ deg/s

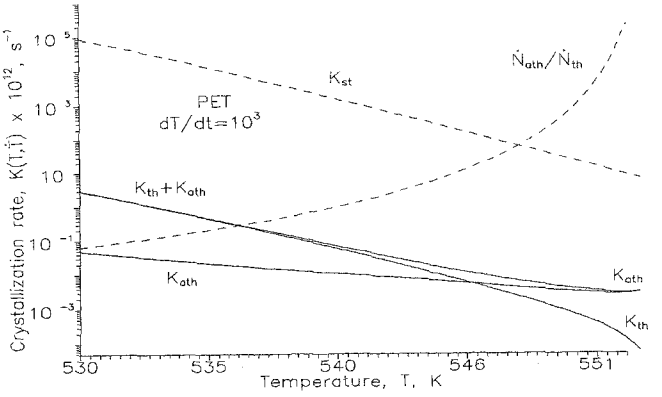

Fig. 8 Steady-state, thermal, athermal, and total crystallization rate components for PET in the vicinity of melting temperature. Cooling rate, $|\dot{T}| = 1000$ deg/s

Athermal nucleation

The ratio of athermal-to-thermal nucleation has been calculated from Eqs. (29) and (30). Figure 6 presents $(\dot{N}_{ath}/\dot{N}_{th})$ plotted vs. crystallization temperature. It is evident that athermal effects for polypropylene are stronger and concentrated in the range of lower temperatures. Since athermal ratio is proportional to $(\Delta T)^{-5}$, very high values appear in the vicinity of melting temperature (481.2 and 553 K, respectively, for polypropylene and PET). Smaller athermal effects in PET may be related to shorter (assumed) relaxation times. It is evident that athermal process provides the only (if any) nucleation mechanism in the vicinity of melting temperature ($\Delta T \to 0$). At high enough cooling rates (smaller for materials with long relaxation times, higher for PET) the ratio $\dot{N}_{ath}/\dot{N}_{th}$ may assume large values, some 10–100 deg below T_m.

Total crystallization rate. Contribution of athermal and relaxational effects

Figure 7 presents temperature dependence of crystallization rate components for polypropylene at a moderate cooling rate, $|\dot{T}| = 10$ deg/s. Similar data for PET at $|\dot{T}| = 1000$ deg/s are shown in Fig. 8. As demonstrated before, strong relaxational effects appear in both polymers in a wide range of temperatures and cooling rates. Athermal effects are much weaker and are limited to temperature region close to melting temperature. Within 1–5 degrees below T_m crystallization in both polymers (if any) is dominated by athermal effects. In polypropylene at $|\dot{T}| = 10$ deg/s (Fig. 7) contribution of athermal crystallization rates is still considerable 40 degrees below T_m. For PET at small cooling rates, athermal effects disappear completely within few degrees below T_m. At a high cooling

rate $|\dot{T}| = 1000$ deg/s (Fig. 8), some athermal effects are visible around 15 deg below T_m.

Thermal crystallization rates in the vicinity of melting temperature are very small (Figs. 7 and 8) and, even if $\mathscr{K}_{ath}$ exceeds $\mathscr{K}_{th}$ by a few orders of magnitude, it is not necessarily true that it will contribute to final crystallinity of the material. The question whether athermal nucleation does affect crystallinity in an industrial process (where polymer is cooled down from the melt to room, or glass transition temperature), requires analysis of the behavior in the range of maximum crystallization rate. The nucleation ratio, $\dot{N}_{ath}/\dot{N}_{th}$ and components of crystallization rate taken at the respective maximum crystallization rate temperatures, T_{max}, have been plotted vs. cooling rate in Figs. 9 and 10. Thermal, athermal, and total crystallization rates have been reduced by the maximum value, K_{max}. It is evident that the actual crystallization rate is considerably smaller than the steady-state values, and the more so, the higher cooling rate is applied. For polypropylene (Fig. 9), deviation of $\mathscr{K}_{tot}$ from $\mathscr{K}_{st}$ can be observed at $|\dot{T}|$ as small as 10^{-4} deg/s; for PET (Fig. 10) at $|\dot{T}| = 10^{-2}$ deg/s $\mathscr{K}_{tot}$ practically coincides with the quasi-static characteristic.

In the case of polypropylene (Fig. 9) athermal contribution appears in a wide range of cooling rates. At $|\dot{T}| = 10$ deg/s, $\mathscr{K}_{ath}$ amounts to ca 21%, and at 1000 deg/s – to ca 72% of the total crystallization rate. For polyethylene terephthalate (with assumed molecular characteristics) significant athermal contribution at T_{max} does not appear below 10^6 deg/s (Fig. 10). At $|\dot{T}| = 10^6$ deg/s, athermal mechanism accounts for 3.5% of crystallization rate, to grow to 66.8% at $|\dot{T}| = 10^8$ deg/s. So high cooling rates do not appear in polymer processing and hardly can be produced in laboratory conditions.

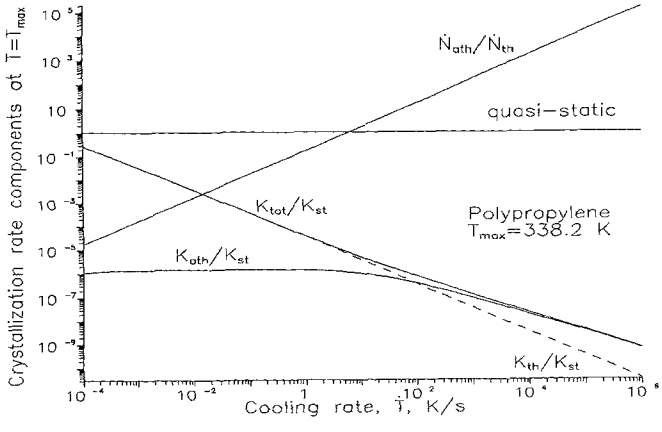

Fig. 9 Components of reduced crystallization rate characteristics for isotactic polypropylene at $T = T_{max}$, vs. cooling rate, $|\dot{T}|$. Solid lines represent: the ratio of athermal to thermal nucleation rate, $\dot{N}_{ath}/\dot{N}_{th}$, reduced athermal, $\mathscr{K}_{ath}$, and total crystallization rate, $\mathscr{K}_{tot} = \mathscr{K}_{th} + \mathscr{K}_{ath}$. The dashed line shows thermal crystallization rate, $\mathscr{K}_{th}$. All crystallization rates are reduced by the maximum crystallization rate, K_{max}

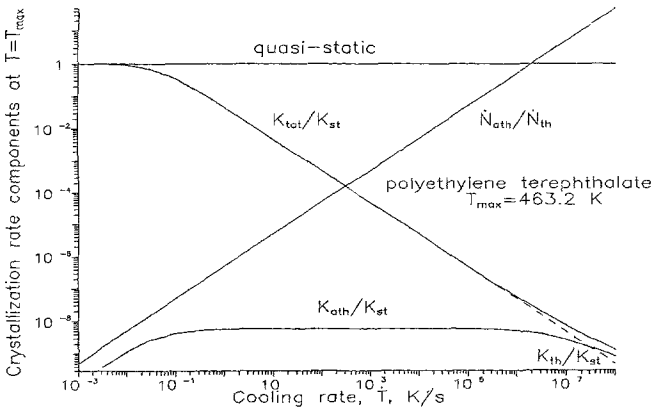

Fig. 10 Components of reduced crystallization rate characteristics of polyethylene terephthalate at $T = T_{max}$, vs. cooling rate, $|\dot{T}|$. Solid lines represent: the ratio of athermal to thermal nucleation rate, $\dot{N}_{ath}/\dot{N}_{th}$, reduced athermal, $\mathscr{K}_{ath}$, and total crystallization rate, $\mathscr{K}_{tot} = \mathscr{K}_{th} + \mathscr{K}_{ath}$. The dashed line shows thermal crystallization rate, $\mathscr{K}_{th}$. All crystallization rates are reduced by the maximum crystallization rate, K_{max}

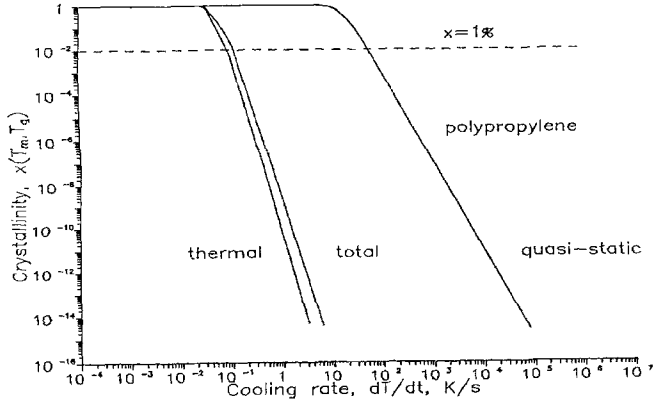

Fig. 11 Components of the degree of transformation (crystallinity), x, for isotactic polypropylene as a function of cooling rate. Solid lines correspond to quasi-static, transient thermal, and total (thermal + athermal) contributions. Dashed line characterizes the minimum level of crystallinity which can be measured ($x = 0.01$)

Figures 11 and 12 present various contributions to crystallinity, x, obtained in non-isothermal processes involving constant cooling rate $|\dot{T}|$. It is evident that total crystallinity resulting from transient thermal and athermal contributions is considerably smaller than a quasi-static one and approaches the latter in the range of very small cooling rates. The difference between total and thermal contributions indicates athermal effects. Taking into account the threshold of measurable fraction of crystalline material ($x = 1\%$), the resulting crystallinity is hardly

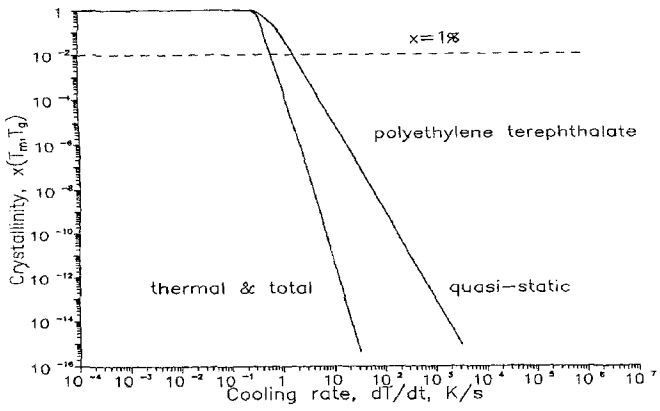

Fig. 12 Components of the degree of transformation (crystallinity), x, for isotactic polypropylene as a function of cooling rate. Solid lines correspond to quasi-static, transient thermal, and total (thermal + athermal) contributions. Dashed line characterizes the minimum level of crystallinity which can be measured ($x = 0.01$). Assumed Avrami exponent $m = 4$

affected by athermal nucleation. This conclusion may be changed when different material properties are considered.

Discussion

The model developed in this paper describes non-isothermal crystallization kinetics in a wide range of temperatures and cooling rates. The model predicts reasonable asymptotic behavior and, combined with reliable material functions: steady-state crystallization rate, $\mathscr{K}_{st}(T)$, relaxation time, $\tau(T)$, and athermal nucleation function, $A_3(T)$, should provide sound basis for quantitative information about crystallization in industrial processes.

Experimental procedures leading to direct determination of the material functions have been outlined. Determination of relaxation time can offer some problems. The method suggested in this paper (Eq. (38)) requires precise measurement of crystallization rate in a *transient isothermal* process. Relaxation times can be measured using a variety of techniques, but it is not clear, what kind of relaxation mechanism is involved in transient crystallization. More studies are needed to elucidate this problem.

Numerical testing of the new model has been based on available molecular and macroscopic parameters. Not all material parameters and functions are fully reliable (e.g. relaxation times) and therefore the results presented in Figs. 1–12 should be considered as qualitative, rather than quantitative. Even if real characteristics are shifted to a different range of conditions, the qualitative picture of non-isothermal crystallization seems to be physically reasonable.

It is evident that *relaxational effects* play an important role in non-isothermal crystallization. Unlike in the quasi-static process, thermal crystallization rate does not follow change of temperatures, but lags behind the steady-state crystallization rate, $\mathscr{K}_{st}(T)$. In the range of high temperatures, $\mathscr{K}_{st}$ increases with undercooling. Increase of the actual crystallization rate is slower, and the more so, the higher is cooling rate, $\dot{T}$. When, in the process of cooling, maximum crystallization rate temperature is reached, steady-state crystallization rate starts to decrease, but the actual crystallization rate levels off, or passes through a flat maximum. Generally speaking, transient crystallization rates (i.e., ones including relaxational effects) are smaller than steady-state rates used in the earlier models of non-isothermal crystallization. Dependently on cooling rates and relaxation times, this reduction can amount to many orders of magnitude.

Athermal effects are much smaller and very sensitive to material characteristics. For isotactic polypropylene, non-isothermal crystallization seems to be affected by athermal nucleation already in the range of small cooling rates ($|\dot{T}| > 10$ deg/s). Athermal effects in polyethylene terephthalate (with material characteristics as assumed in Table 1) are confined to temperatures very close to melting temperature and/or extremely high cooling rates $|\dot{T}| > 10^6$ deg/s. Even if athermal nucleation does not contribute to final degree of crystallinity (Figs. 11 and 12) the number of athermal nuclei produced in the system, may affect secondary crystallization of samples subjected to rapid cooling.

As mentioned above, numerical calculations have been based on rather incomplete and uncertain material data, and therefore can be considered as *qualitative*. Experimental determination of the basic material functions is necessary for any reliable, *quantitative* predictions.

Acknowledgment This work has been supported in part by Research Grant # PB 1291/S2/93/04 offered by the Committee of Scientific Research (Komitet Badań Naukowych).

Appendix A

Basic equations of the nucleation theory [7, 8]

More recent theories of crystal nucleation consider anisotropic clusters whose configuration is described by many variables characterizing size and shape; thermodynamic properties of such clusters involve surface energy density, different for different crystal faces [8]. For the sake of simplicity, we will consider a reduced model of nucleation close to the original treatment [7] in which cluster size is characterized by a single variable, g (cluster size), and one

Colloid & Polymer Science, Vol. 274, No. 8 (1996)

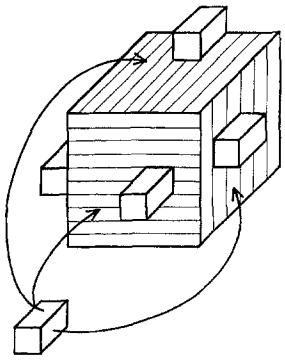

Fig. A1 Scheme of three-dimensional (primary) nucleation. Single kinetic elements are attached to all faces of the growing cluster

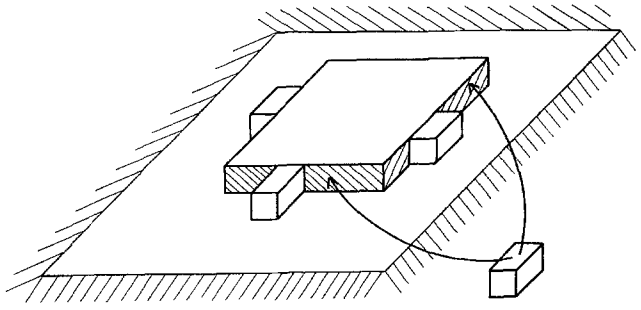

Fig. A2 Scheme of two-dimensional (secondary) nucleation. The cluster forms monomolecular layer on crystal surface and grows in the lateral directions

average surface energy characteristic, σ. This model describes isotropic clusters, or anisotropic clusters which, during their growth maintain constant, thermodynamically most probable shape, with minimum free energy.

Two types of nucleation will be considered: three-dimensional, bulk nucleation, leading to primary crystal nuclei (Fig. A1), and two-dimensional, surface nucleation, responsible for nucleation-controlled growth (Fig. A2). In subsequent formulas, individual cases are marked by subscript "i" ($i = 2, 3$).

Free energy of the transition of g single kinetic elements, each of volume v_0, into an i-dimensional, g-size cluster consists of bulk and surface contributions

$$\Delta\tilde{F}_i(g) = -\Delta h(\Delta T/T_m)v_0 g + c_i\sigma_i v_0^{2/3} g^{(i-1)/i}\,, \tag{A1}$$

where c_i is a shape factor. For a parallelepiped $c_2 = 4$, and $c_3 = 6$. Δh denotes heat of fusion, $\Delta T = T_m - T$ is undercooling, σ_i average surface energy density. In the case of isotropic clusters, there appears only one interface tension: $\sigma = \sigma_s = \sigma_e$, and, consequently $\sigma_2 = \sigma_3 = \sigma$. For proportionally growing anisotropic clusters with axial symmetry, two different surface energy densities are involved: σ_e on the surface normal to symmetry axis, and σ_s on the parallel surface. It can be shown that the effective average values appearing in Eq. (A1) read: $\sigma_2 = \sigma_s$ (growth in the direction of the symmetry axis), $\sigma_2 = (\sigma_e\sigma_s)^{1/2}$ (lateral growth), and $\sigma_3 = (\sigma_e\sigma_s^2)^{1/3}$ (bulk growth).

Critical size defining stable clusters (nuclei) is obtained from the condition:

$$g = g_i^*: \qquad \frac{\partial\Delta F_i}{\partial g} = 0 \tag{A2}$$

It is easy to show that

$$g_i^* = \left[\frac{(i-1)c_i\sigma_i T_m}{i\cdot\Delta h\,\Delta T\, v_0^{1/3}}\right]^i \tag{A3}$$

$$\frac{dg_i^*}{dT} = \frac{i\,g_i^*}{\Delta T} = \frac{i}{\Delta T}\left[\frac{(i-1)c_i\sigma_i T_m}{i\cdot\Delta h\,\Delta T\, v_0^{1/3}}\right]^i . \tag{A4}$$

Maximum free energy providing thermodynamic part of the potential barrier for nucleation results in the form:

$$\Delta\tilde{F}_i^* = \Delta\tilde{F}_i(g_i^*) = \frac{1}{i}c_i\sigma_i v_0^{2/3}\left[\frac{(i-1)c_i\sigma_i T_m}{i\cdot\Delta h\,\Delta T\, v_0^{1/3}}\right]^{i-1} . \tag{A5}$$

It is evident that for three-dimensional, primary nuclei ($i = 3$), critical cluster size g^* is proportional to $(\Delta T)^{-2}$; for secondary (surface) nuclei ($i = 2$) $g^* \propto (\Delta T)^{-3}$. Similarly, maximum free energy (thermodynamic barrier for nucleation), $\Delta\tilde{F}^*$, is proportional to $(\Delta T)^{-2}$ for primary nuclei, and to $(\Delta T)^{-1}$ for secondary nuclei.

In the simplified nucleation theory, cluster size distribution, $\varrho_i(g, t)$, is determined by the kinetic (Fokker–Planck) equation

$$\frac{\partial\varrho_i}{\partial t} - \frac{\partial}{\partial g}\left[\mathscr{D}_{gr,i}\left(\frac{\partial\varrho_i}{\partial g} + \frac{\varrho_i}{kT}\frac{\partial\Delta\tilde{F}_i}{\partial g}\right)\right] = 0; \quad i = 2, 3\,. \tag{A6}$$

The growth-diffusion coefficient, $\mathscr{D}_{gr,i}$ is equal to the dissociation rate coefficient, k_i^- [8]

$$\mathscr{D}_{gr,i} = k_i^-(T, g) = \nu\exp[-E_a/kT]\,(c_i g^{(i-1)/i})\,, \tag{A7}$$

where ν is basic frequency of molecular motions enabling association–dissociation reactions, c_i is a dimensionless shape factor (identical to that in Eq. A1), and E_a – activation energy for diffusional transport of single kinetic elements to and from cluster surface. The g-dependent term accounts for the number of sites on cluster surface available for dissociation.

According to the theory of chemical reaction rates [9], the frequency ν is proportional to absolute temperature and reads

$$\nu = kT/h\,, \tag{A8}$$

where k and h denote, respectively, Boltzmann and Planck constants.

For large clusters, free energy of aggregation does not contribute to the dissociation barrier, and only the transport barrier, E_a, appears in Eq. (A7) (cf. ref. [10]).

The transport activation term can be related to molecular mobility and relaxation time, τ

$$\tau = \tau_0 \exp[E_a/kT] \tag{A9}$$

which, combined with Eq. (A7) yields

$$\mathscr{D}_{gr,i} = D_{0,i}\, g^{(i-1)/i} \tau^{-1} \tag{A10}$$

and

$$D_{0,i} = \frac{kT}{h} \tau_0 c_i \,. \tag{A11}$$

In the case of primary nuclei ($i = 3$), aggregation rate is proportional to cluster surface ($g^{2/3}$); in the case of secondary nuclei ($i = 2$) – to cluster periphery ($g^{1/2}$).

Integration of the steady-state kinetic equation ($\partial \varrho_i/\partial t = 0$), with boundary conditions:

$$\begin{aligned} &\varrho_i(g = 1) = C_{0,i} \\ &\varrho_i(g = G \gg g^*) = 0 \end{aligned} \tag{A12}$$

yields steady-state distributions

$$\varrho_{st,i}(g) = C_{0,i}\, e^{-\Delta\tilde{F}_i/kT} \frac{\int_g^G (e^{-\Delta\tilde{F}_i/kT}/\mathscr{D}_{gr,i})\,dg}{\int_1^G (e^{\Delta\tilde{F}_i/kT}/\mathscr{D}_{gr,i})\,dg} \tag{A13}$$

$$\frac{\partial \varrho_{st,i}}{\partial g} = -C_{0,i} \times \frac{(\Delta\tilde{F}_i'/kT)\, e^{-\Delta\tilde{F}_i/kT} \int_g^G (e^{-\Delta\tilde{F}_i/kT}/\mathscr{D}_{gr,i})\,dg + 1/\mathscr{D}_{gr,i}}{\int_1^G (e^{\Delta\tilde{F}_i/kT}/\mathscr{D}_{gr,i})\,dg} \,, \tag{A14}$$

where $C_{0,i}$ is a constant. The solution assumes a simple form at $g = g_i^*$. First derivative of the free energy, $(\partial \Delta\tilde{F}_i/\partial g)$, disappears. The kernels of integrals appearing in Eqs. (A13)–(A14) exhibit maxima in the vicinity of g_i^*, and can be approximated by

$$\ln[e^{\Delta\tilde{F}_i/kT}/\mathscr{D}_{gr,i}] \simeq \frac{\Delta\tilde{F}_i(g_i^*)}{kT} - \ln \mathscr{D}_{gr,i}(g_i^*) - \frac{(i-1)(g-g_i^*)}{i g_i^*} + \mathscr{O}[(g-g_i^*)^2] \,. \tag{A15}$$

The upper integration limit, G, is always large compared with g_i^*, and can be replaced with infinity. The approximate integrals assume the form

$$\begin{aligned} \int_1^G (e^{\Delta\tilde{F}_i/kT}/\mathscr{D}_{gr,i})\,dg &\simeq \int_1^\infty (e^{\Delta\tilde{F}_i/kT}/\mathscr{D}_{gr,i})\,dg \\ &\simeq \frac{i g_i^*}{(i-1)} \exp\left[\frac{(i-1)(g_i^*-1)}{i g_i^*}\right] (e^{\Delta\tilde{F}_i/kT}/\mathscr{D}_{gr,i})_{g=g_i^*} \\ &\simeq \frac{i g_i^*}{(i-1)} e^{(i-1)/i} (\mathscr{D}_{gr,i}^*)^{-1} \exp[\Delta\tilde{F}_i^*/kT] \end{aligned} \tag{A16}$$

$$\begin{aligned} \int_{g^*}^G (e^{\Delta\tilde{F}_i/kT}/\mathscr{D}_{gr,i})\,dg &\simeq \int_{g^*}^\infty (e^{\Delta\tilde{F}_i/kT}/\mathscr{D}_{gr,i})\,dg \\ &\simeq \frac{i g_i^*}{(i-1)} (\mathscr{D}_{gr,i}^*)^{-1} \exp[\Delta\tilde{F}_i^*/kT] \,. \end{aligned} \tag{A17}$$

Substitution of the approximated integrals into the steady-state distribution yields

$$\varrho_{st,i}(g_i^*) \simeq C_{0,i} e^{-(i-1)/i} \exp[-\Delta\tilde{F}_i^*/kT] \tag{A18}$$

$$\left.\frac{\partial \varrho_{st,i}}{\partial g}\right|_{g=g_i^*} \simeq -C_{0,i} \frac{i-1}{i g_i^*} e^{-(i-1)/i} \exp[-\Delta\tilde{F}_i^*/kT] = -\frac{i-1}{i g_i^*} \varrho_{st,i}(g_i^*) \,. \tag{A19}$$

The number of stable (supercritical) clusters existing in the system at the instant, t, is given by the integral

$$N_i(t) = \int_{g_i^*}^G \varrho_i(g, t)\,dg \,. \tag{A20}$$

Differentiation of Eq. (A20) with respect to time yields *nucleation rate*, i.e., production rate of stable clusters

$$\dot{N}_i(t) = dN_i/dt = \dot{N}_{th,i} + \dot{N}_{ath,i} \,. \tag{A21}$$

The first term, *thermal nucleation*, provides a flux of clusters through the potential barrier $\Delta\tilde{F}_i^*$

$$\dot{N}_{th,i} = -\mathscr{D}_{gr,i}(g_i^*) \left.\frac{\partial \varrho_i}{\partial g}\right|_{g=g_i^*} \,. \tag{A22}$$

The second term, *athermal nucleation*, appears in nonisothermal conditions as a result of time-dependent critical cluster size g_i^*

$$\dot{N}_{ath,i} = -(dg_i^*/dt)\varrho_i(g_i^*) \,. \tag{A23}$$

Application of the approximate steady-state distribution (A18) and Eq. (A10) yields

$$\begin{aligned} \dot{N}_{th,st,i} &\simeq C_{0,i} \frac{i-1}{i} e^{-(i-1)/i} D_{0,i}(g_i^*)^{-1/i} \tau^{-1} \exp[-\Delta\tilde{F}_i^*/kT] \\ &= C_{0,i} e^{-(i-1)/i} \frac{kT}{h} \frac{\Delta h\, \Delta T\, v_0^{1/3}}{\sigma_i T_m} \exp[-E_a/kT] \\ &\quad \times \exp[-\Delta\tilde{F}_i^*/kT] \end{aligned} \tag{A24}$$

$$\dot{N}_{\mathrm{ath,st,i}} \simeq -C_{0,\mathrm{i}} e^{-(\mathrm{i}-1)/\mathrm{i}} \dot{T}(dg_{\mathrm{i}}^*/dT)\exp[-\Delta\tilde{F}_{\mathrm{i}}^*/kT]$$
$$= -C_{0,\mathrm{i}} \frac{i\dot{T}}{\Delta T} e^{-(\mathrm{i}-1)/\mathrm{i}} \exp[-\Delta\tilde{F}_{\mathrm{i}}^*/kT]$$
$$\times \left[\frac{(i-1)c_{\mathrm{i}}\sigma_{\mathrm{i}}T_{\mathrm{m}}}{i\cdot\Delta h\,\Delta T\,v_0^{1/3}}\right]^{\mathrm{i}} \quad \text{(A25)}$$

where $\dot{T} = dT/dt$, is cooling rate.

The ratio of athermal to thermal nucleation rates, based on the approximate distribution, results as

$$(\dot{N}_{\mathrm{ath,st}}/\dot{N}_{\mathrm{th,st}})_{\mathrm{i}} = u\cdot A_{\mathrm{i}} \simeq -\frac{\dot{T}\tau}{\Delta T}\frac{i^{1-\mathrm{i}}(i-1)^{\mathrm{i}}}{D_{0,\mathrm{i}}}\left[\frac{c_{\mathrm{i}}\sigma_{\mathrm{i}}T_{\mathrm{m}}}{\Delta h\,\Delta T\,v_0^{1/3}}\right]^{\mathrm{i}+1}$$
$$= -\frac{\dot{T}\tau}{T}\frac{h\,i^{1-\mathrm{i}}(i-1)^{\mathrm{i}}}{\tau_0 k\,\Delta T}(c_{\mathrm{i}})^{\mathrm{i}}\left[\frac{\sigma_{\mathrm{i}}T_{\mathrm{m}}}{\Delta h\,\Delta T\,v_0^{1/3}}\right]^{\mathrm{i}+1}$$
$$-\frac{\dot{T}h}{kT\,\Delta T}\,i^{1-\mathrm{i}}(i-1)^{\mathrm{i}}(c_{\mathrm{i}})^{\mathrm{i}}\left[\frac{\sigma_{\mathrm{i}}T_{\mathrm{m}}}{\Delta h\,\Delta T\,v_0^{1/3}}\right]^{\mathrm{i}+1}$$
$$\times\exp[E_{\mathrm{a}}/kT]\,. \quad \text{(A26)}$$

Temperature dependence of thermal nucleation rate can thus be presented in the form:

$$\dot{N}_{\mathrm{th,st,3}} = K_3\cdot(T\Delta T/T_{\mathrm{m}}^2)\exp[-E_{\mathrm{a}}/kT]$$
$$\times\exp[-C_3 T_{\mathrm{m}}^3/T\Delta T^2] \quad \text{(A27)}$$

for primary, three-dimensional nucleation, and

$$\dot{N}_{\mathrm{th,st,2}} = K_2\cdot(T\Delta T/T_{\mathrm{m}}^2)\exp[-E_{\mathrm{a}}/kT]$$
$$\times\exp[-C_2 T_{\mathrm{m}}^2/T\Delta T] \quad \text{(A28)}$$

for secondary, two-dimensional nucleation. Values of the dimensionless constants K_2, K_3, C_2, C_3 are shown in Table A1.

Table A1 Constants in steady-state nucleation rates

	Primary nucleation, $i = 3$	Secondary nucleation, $i = 2$
K_{i}	$C_{0,3}e^{-2/3}\frac{kT_{\mathrm{m}}\Delta h v_0^{1/3}}{h\sigma_3}$	$C_{0,2}e^{-1/2}\frac{kT_{\mathrm{m}}\Delta h v_0^{1/3}}{h\sigma_2}$
C_{i}	$\frac{4}{27}\frac{(c_3\sigma_3)^3}{kT_{\mathrm{m}}\Delta h^2}$	$\frac{1}{4}\frac{(c_2\sigma_2)^2 v_0^{1/3}}{kT_{\mathrm{m}}\Delta h}$
σ_{i}	$(\sigma_{\mathrm{e}}\sigma_{\mathrm{s}}^2)^{1/3}$	$(\sigma_{\mathrm{e}}\sigma_{\mathrm{s}})^{1/2}$
c_{i}	6	4

References

1. Ziabicki A (1995) Colloid Polym Sci 273: 209
2. Kolmogoroff AN (1937) Izvestiya Akad Nauk SSSR, Ser Math: 3:335
3. Avrami M (1939) J Chem Phys 7:1103
4. Johnson WA, Mehl RF, Trans AIME 135, 416 (1939)
5. Evans UR (1945) Trans Faraday Soc 41: 365
6. Ziabicki A (1967) Appl Polymer Symposia 6:1
7. Turnbull D, Fisher JC (1949) J Chem Phys 17:71
8. Ziabicki A (1986) J Chem Phys 85:3042
9. Glasstone S, Laidler K, Eyring H (1947) The Theory of Rate Processes, McGraw & Hill, New York
10. Ziabicki A, Jarecki L (1984) J Chem Phys 80:5751
11. Williams ML, Landel RF, Ferry JD (1955) J Am Chem Soc 77:3701
12. Ziabicki A, Fundamentals of Fibre Formation, Wiley, London, 1976
13. Monasse B, Haudin JM (1986) Colloid Polym Sci 264:117
14. Palys LH, Phillips PJ (1980) J Polym Sci (Phys) 18:829
15. Cobbs WH, Burton RL (1953) J Polym Sci 50:275
16. Magill JH (1962) Polym, 3:35
17. Alfonso GC, Ziabicki A (1995) Colloid Polym Sci 273:317
18. Billingham N, Calvert PD, Uzuner A (1990) Polym 31:258
19. Cappuccio V, Coen A, Bertinotti F (1962) Chim Ind (Milano) 44:463